

Physical and discrete element models of excavation and failure in jointed rock

Nick Barton

Norwegian Geotechnical Institute, Oslo, Norway

Abstract:

Physical models of single joints, of rock masses and of model excavations in rock can sometimes provide important insights into potential behaviour and failure modes in real rock masses. They can also provide verification or validation of computer codes. However, where failure or large strains are concerned, the computer models that are based on isotropic continuum behaviour will usually fall short of reality. Discrete element models with realistic constitutive laws for the joints may, on the other hand, provide good simulations of the physical behaviour seen in physical models, and therefore appear likely to be able to simulate or predict real behaviour. An example of a virtual validation of the UDEC-BB discrete element code with results from a well instrumented large excavation are given to illustrate this point. A unifying theme that runs through the article is the importance of shear induced dilation and associated joint roughness. This prime parameter helps rock masses to accommodate the "key" blocks and "plastic" zones that we sometimes all too eagerly predict when ignoring the rock block and rock mass interlock effect. The exact opposite is experienced with the low- J_r and high- J_a discontinuity that causes rock support needs to escalate due to non-dilatant or even contractile behaviour, when such a feature tries to resist but actually causes failure. The interlock of the surrounding rock joints may be seriously compromised by such features, and raveling may result.

1. PHYSICAL MODELS OF ROCK JOINTS

Physical models of rock joints, rock masses and excavations in rock have much to offer in rock mechanics. As a starting point, some of the things we have learned from studies of model rock joints will be considered.

Direct shear tests of tension fractures that were developed in a range of weak model materials are shown in Fig. 1. What appeared at the time to be alarmingly high peak friction angles (ϕ_p) proved later to be a fundamental feature of non-planar rock joints. It appears that if a shear test is conducted at low enough normal stress, ϕ_p may tend to be as high as 90° , as shown in the inset to Fig. 1.

As explained by Barton and Bandis (1990), the rough tension fractures depicted in Fig. 1 represent valid "end members" of the family called rock joints. In the terminology JRC, JCS and ϕ_r developed by Barton and Choubey (1977) to extrapolate tilt test results, the tension fracture has the highest possible JRC, JCS and ϕ_r values.

2. CONSTITUTIVE MODELS FOR THE SHEAR STRENGTH OF ROCK JOINTS

For the model tension fractures discussed above, linear plots of peak friction angle ($\arctan \tau/\sigma_n$) vs peak dilation angle (d_n) indicated the following simple expression:

$$\tau = \sigma_n \tan (2d_n + 30^\circ) \quad (1)$$

It was found that the peak dilation angle was proportional to the logarithm of the ratio (σ_c/σ_n) (compression strength/normal stress):

$$d_n = 10 \log \left(\frac{\sigma_c}{\sigma_n} \right) \quad (2)$$

By elimination, the following simple form was obtained:

$$\tau = \sigma_n \tan \left[20 \log \left(\frac{\sigma_c}{\sigma_n} \right) + 30^\circ \right] \quad (3)$$

Thus the first form of the "JRC-JCS" model was actually the "20 - σ_c " model, where the roughness

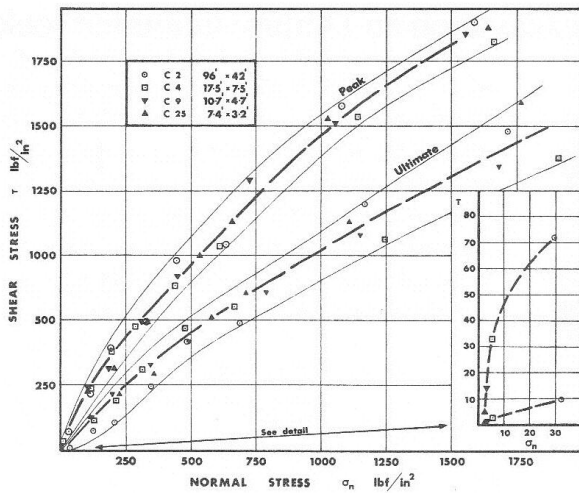


Fig. 1. Tension fractures in model materials demonstrate an important extreme value of ϕ_p at low stress (Barton, 1971).

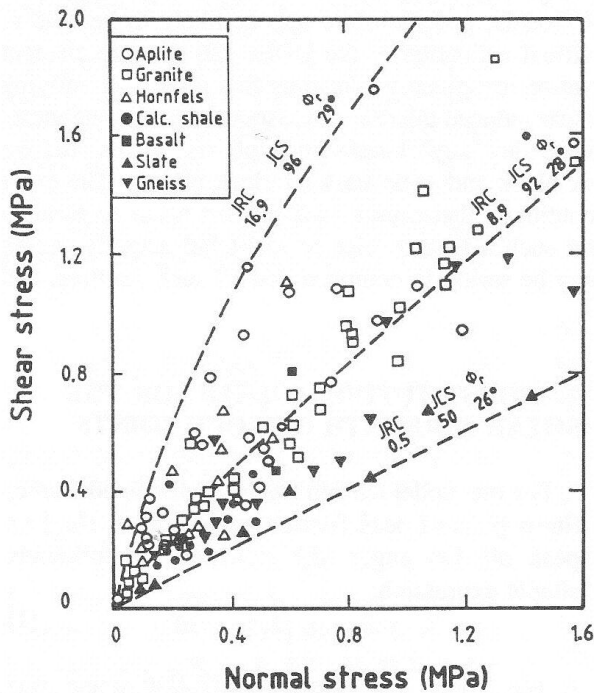


Fig. 2. Peak shear strength of 130 rock joints and strength prediction with equation 4.

coefficient (JRC) was equal to 20 for these rough tension fractures. The joint wall strength (JCS) was equal to σ_c (the unconfined compression strength). The original form (equation 3) is therefore perfectly consistent with today's equation:

$$\tau = \sigma_n \tan \left[JRC \log \left(\frac{JCS}{\sigma_n} \right) + \phi_r \right] \quad (4)$$

Equation 3 represents the three limiting values of the three input parameters, i.e.,

JRC = 20 (roughest possible joint without actual steps)

JCS = σ_c (least possible weathering grade, i.e., fresh fracture)

$\phi_r = \phi_b$ (fresh unweathered fracture with basic friction angles in the range $28\frac{1}{2}$ to $31\frac{1}{2}$ °)

The small size of the model tension fractures (60mm length) meant that both JRC and JCS were truly laboratory scale parameters and would nowadays be given the subscripts JRC₀ and JCS₀ Barton et al., 1985) to distinguish them from the scale-corrected full scale values JRC_n and JCS_n (see later).

3. PEAK STRENGTH OF ROCK JOINTS AND ITS PREDICTION

Fig. 2 illustrates the results of direct shear tests, on 130 rock joints, reported by Barton and Choubey (1977). Eight rock types were represented. The mean values of the above shear strength parameters were as follows:

$$JRC = 8.9 \quad JCS = 92 \text{ MPa} \quad \phi_r = 28^\circ$$

These values were used as input parameters in equation 4 to derive the central strength envelope in Fig. 2. A key aspect of this study was the discovery that self-weight tilt testing, such as illustrated in Fig. 3, could be used to predict peak shear strength.

The tilt tested laboratory joint sample generally reaches failure when the normal stress is as low as 0.001 MPa. Remarkably, equation 4 gives a reasonably accurate estimate of peak friction angle up to normal stress levels approaching five orders of magnitude higher.

At stress levels approaching the level of σ_c (or JCS), substitution of the confined strength ($\sigma_1 - \sigma_3$) in equation 4 in place of σ_c (or JCS) gives a very good fit to the shear strength of fresh fractures. Asperities apparently develop higher strength due to their increased confinement with the greater areas of contact (Barton, 1976):

$$\tau = \sigma_n \tan \left[JRC \log \left(\frac{\sigma_1 - \sigma_3}{\sigma_n} \right) + \phi_r \right] \quad (5)$$

The logarithmic form of equations 4 and 5 means that the peak friction angle increases by JRC degrees for every order of magnitude reduction in normal stress.

Table 1 illustrates this with example values of $JRC = 5$ and 10 , and $JCS = 100$ MPa. Typical tilt angles (α°) at failure would be expected to be about 55° and 80° respectively. Since tilt angles approaching 90° present experimental difficulties (toppling before sliding) and theoretical difficulties (cohesion intercept), the use of tilt tests for joints with JRC values greater than about 10 is generally impossible and horizontal pull tests must be used. The general formula for evaluating tilt tests is:

$$JRC = \frac{\alpha^\circ - \phi_r^\circ}{\log \left[\frac{JCS}{\sigma_n} \right]} \quad (6)$$

4. DILATION OF ROCK JOINTS AND ITS PREDICTION

Asperity angles (i) of about 60° will be sufficient to give rock joints true cohesion intercepts, and will tend to prevent tilt testing. In effect the joint experiences a peak dilation angle of equal magnitude to the (i) value. Peak dilation angles recorded in the direct shear tests shown in Fig. 2 varied from 0° to 60° with an average value of 20.0° . At low normal stress levels, with little asperity damage, the peak dilation angle can be approximated by:

$$d_n = JRC \log \left(\frac{JCS}{\sigma_n} \right) \quad (7)$$

At higher normal stress, with increasing asperity damage the peak dilation angle may reduce to as low as

Table 1. Effect of large stress changes on peak friction angles for example values of $JRC = 5$ or 10 , $JCS = 100$ MPa and $\phi_r = 30^\circ$. ($\dagger JCS \rightarrow \sigma_1 - \sigma_3$, \ddagger typical for tilt tests)

σ_n (MPa)	arctan (τ/σ_n)	arctan (τ/σ_n) $^\circ$	
		JRC=5	JRC=10
100 \dagger	$> \phi_r$	$> 30^\circ$	$> 30^\circ$
10	$\phi_r + JRC$	35°	40°
1	$\phi_r + 2 JRC$	40°	50°
0.1	$\phi_r + 3 JRC$	45°	60°
0.01 \ddagger	$\phi_r + 4 JRC$	50°	70°
0.001 \ddagger	$\phi_r + 5 JRC$	55°	80°

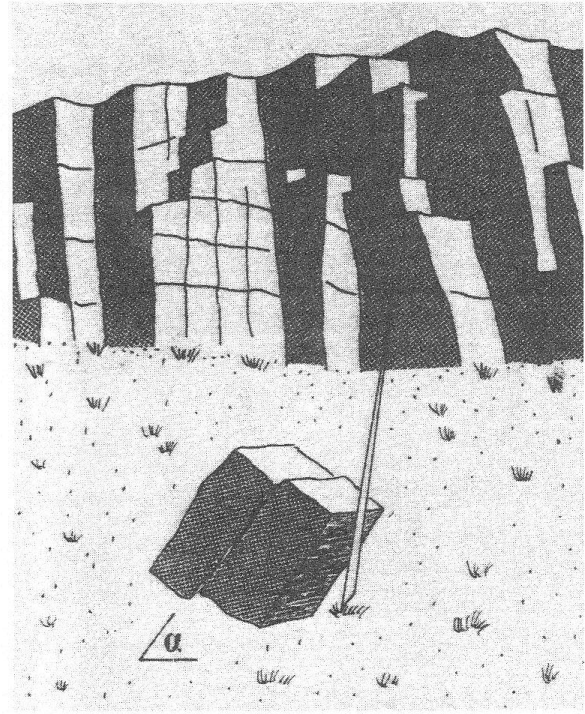


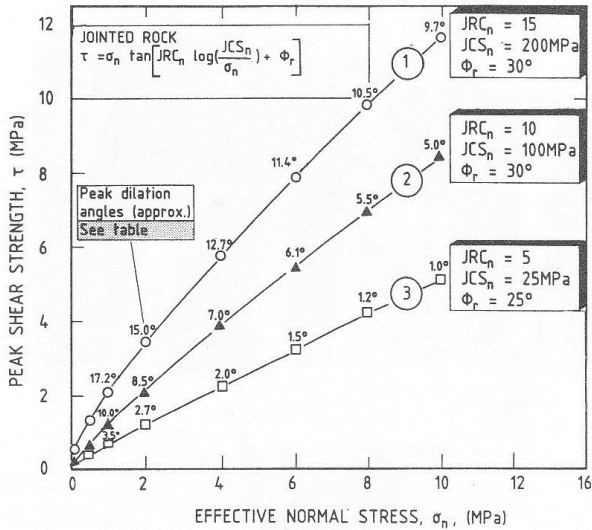
Fig. 3. Tilt test for JRC and ϕ_b .

$$d_n = \frac{1}{2} JRC \log \left(\frac{JCS}{\sigma_n} \right) \quad (8)$$

To illustrate the importance of dilation angles to the behaviour of rock joints in confined situations, the strength envelopes drawn in Fig. 4 have been appended the minimum likely values of d_n (from equation 8). It is likely that the dilation angles are even higher for envelope 1 thereby emphasising the great importance of both joint roughness and joint wall strength in the stability of underground openings. Ignoring such factors in key block analyses can lead to over-conservative design of reinforcement. Plastic zones may be seriously over-predicted for similar reasons.

5. MODELS OF SHEAR STRESS AND DISPLACEMENT BEHAVIOUR

The direct shear tests of model tension fractures shown in Fig. 1 were performed in the normal manner, with continuous recording of shear resistance and normal and shear displacement. From this data the author developed the concept of mobilised roughness (JRC_{mob}) so that shear stress-displacement curves could be predicted or modelled. Fig. 5 shows a dimensionless plot of the direct shear tests performed on these model tension



Estimates of peak dilation angles (d_h^p)

Curve no.	Effective normal stress (MPa)								
	0.1	0.5	1.0	2.0	4.0	6.0	8.0	10.0	
1	24.7	19.5	17.2	15.0	12.7	11.4	10.5	9.7	
2	15.0	11.5	10.0	8.5	7.0	6.1	5.5	5.0	
3	6.0	4.2	3.5	2.7	2.0	1.5	1.2	1.0	

Fig. 4. Peak dilation angles appended to shear strength envelopes (Barton, 1987).

fractures which had JCS ($= \sigma_c$) = 0.4 MPa, and JRC = 20.

Equation 4 was rearranged so that the joint roughness mobilized at any displacement could be back-calculated:

$$JRC_{(mob)} = \frac{\arctan\left(\frac{\tau_m}{\sigma_n}\right) - \phi_r}{\log_{10}\left(\frac{JCS}{\sigma_n}\right)} \quad (9)$$

where τ_m = shear strength mobilized at any displacement.

Equation 9 was evaluated at several points along each of the shear force-displacement curves. Data was then normalised to the form $JRC_{(mob)}/JRC_{(peak)}$ and $\delta_h/\delta_{h(peak)}$, where $\delta_{h(peak)}$ was the displacement required to reach peak strength under the particular test. These dimensionless data are shown in Fig. 5.

As a direct result of these earlier physical model tests it was now possible to develop a constitutive model for predicting the shear-stress displacement (and dilation) curves of rock joints. The proposed general form of this $JRC_{(mob)}$ model is shown in Fig. 6 (Barton, 1982).

The constitutive model shown in Fig. 6 has been tested against cast model replicas of rock joints that were developed and direct shear tested by Bandis

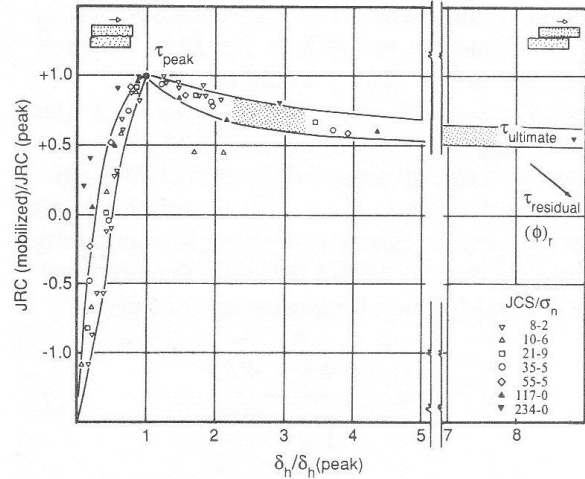


Fig. 5. Dimensionless shear strength - displacement curves for model tension fractures (Barton and Hansteen, 1979).

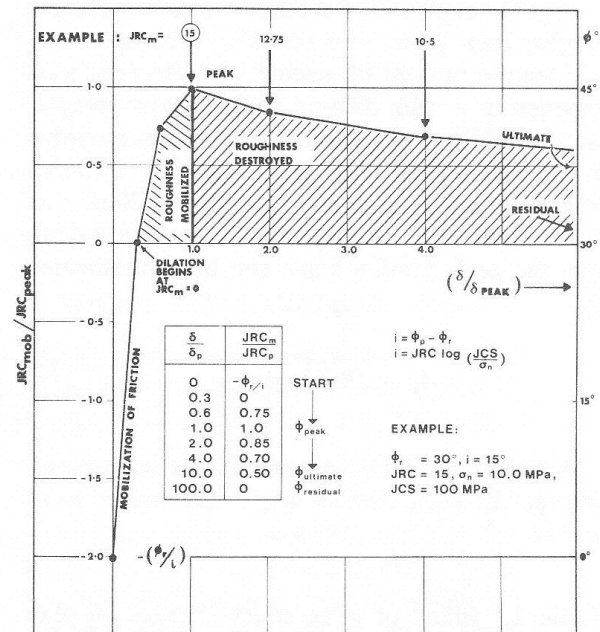


Fig. 6. Dimensionless model for predicting shear stress-displacement behaviour of rock joints.

(1980). An example of the good fit between the physical model tests and the constitutive model prediction is illustrated in Fig. 7.

6. PHYSICAL MODELS OF JOINTED ROCK MASSES TO STUDY SCALE EFFECTS

Although often idealised to two-dimensions, physical models have provided valuable insight into

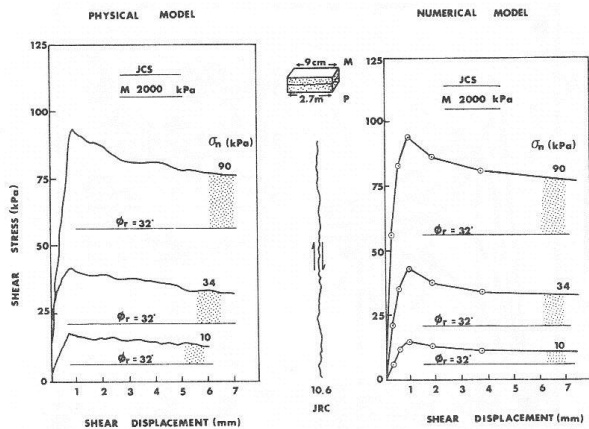


Fig. 7. Comparison of Bandis (1980) model joint replicas and the shear strength-displacement predictions of the $JRC_{(mob)}$ model (Barton, 1982).

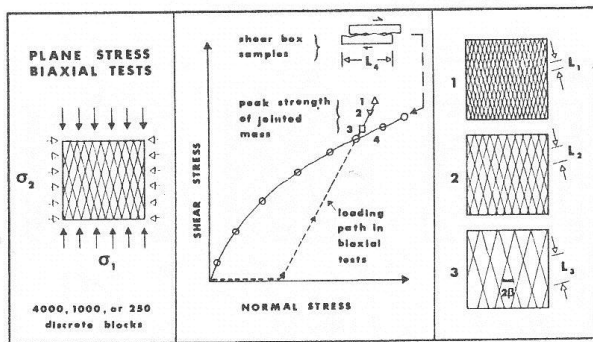


Fig. 8. Tension fracture models of rock masses indicate higher shear resistance with small block sizes (Barton and Bandis, 1982).

the behaviour of jointed rock masses. Ladanyi and Archambault (1972), Hoek (1983) and Barton and Hansteen (1979) have described studies of failure modes and of block-size scale effects. The results shown in Fig. 8 indicate that rock masses consisting of very small blocks, although likely to be more deformable, will tend to have higher shear resistance than rock masses consisting of larger blocks, all other factors being held constant (identical methods of generating the tension fractures). Because of the model scale, the direct shear test sample lengths (L_4) shown in Fig. 8 are larger than the three block sizes (L_1 to L_3) investigated as block assemblies.

Evidence from tilt tests of rock joints of different size (Barton and Choubey, 1977) confirm such experiences, and constitute some of the data needed to scale the values of JRC_0 and JCS_0 obtained for

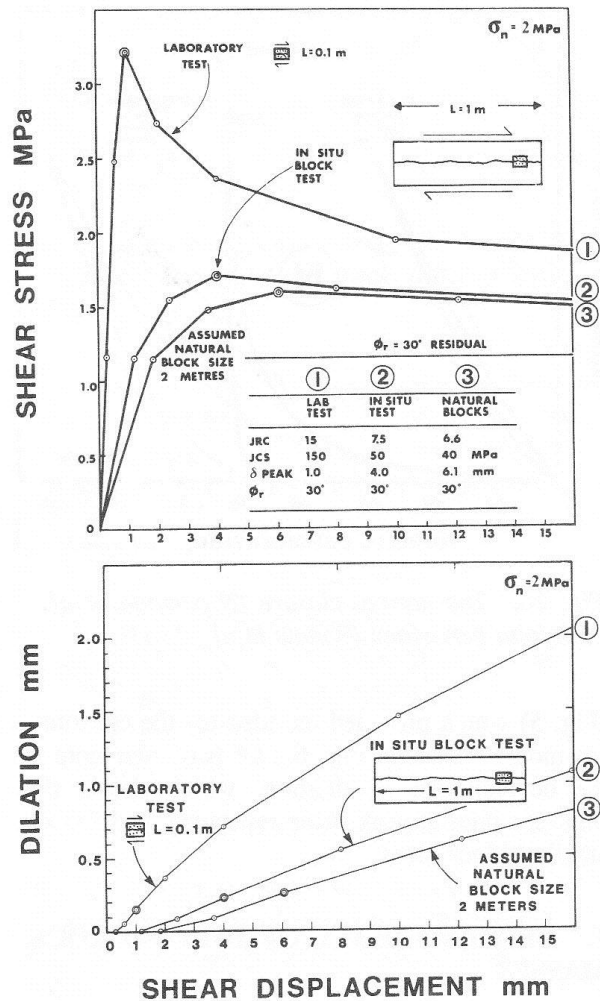


Fig. 9. Constitutive model prediction of stress-displacement and dilation-displacement behaviour of rock joints of different size (Barton, 1982)

laboratory samples, to the values JRC_n and JCS_n for larger sized blocks. The two equations given below show how JRC and JCS given in Equation 4 can be scaled down to allow for the lower shear resistance found at *in situ* block size.

$$JRC_n \approx JRC_0 \left(\frac{L_n}{L_0} \right)^{-0.02 JRC_0} \quad (10)$$

$$JCS_n \approx JCS_0 \left(\frac{L_n}{L_0} \right)^{-0.03 JRC_0} \quad (11)$$

Examples of the magnitude of scale effects that can be expected over the early shear stress-displacement field are given in Fig. 9 for three different hypothetical block sizes. The predicted behaviour is developed via our physical model studies

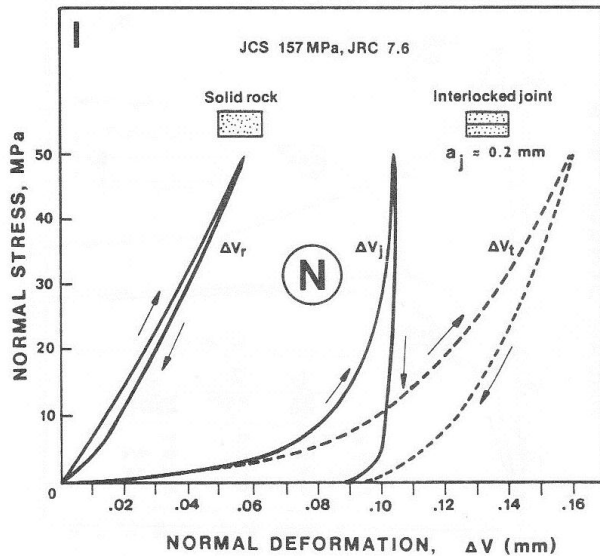


Fig. 10. The normal closure (*N* component of rock joint behaviour (Bandis et al., 1983)

(Fig. 5) which provided the idea for the constitutive model shown in Fig. 6. Of particular note is the development of dilation, which shows the highest values at peak shear resistance, and for the smallest block sizes.

7. DEFORMABILITY OF JOINTED ROCK MASSES

The fundamental components of rock joint deformability, namely closure and shearing (often accompanied by dilation) are shown in Figs 10 and 11. These normal (*N*) and shear (*S*) components are combined in hypothetical rock mass models in Fig. 12.

The general shapes of the curves in this figure are similar to those obtained in plate loading and block tests of rock mass response, as described by Rocha (1964), Hardin et al. (1981) and Hart et al. (1985).

Tests of these hypotheses have been reported by Chryssanthakis et al. (1991), using the discrete element UDEC model (Cundall, 1980) with the Barton-Bandis (BB) constitutive behaviour described earlier. In the one-dimensional strain loading that was simulated, the Type A rock mass (Fig. 12) showed the lowest displacement, joint shear and maximum stress (11 MPa), while the Type C rock mass showed the highest displacement (1.75mm), joint shear (0.24mm) and maximum stress (32 MPa). The "basalt" (Type B) showed intermediate behaviour.

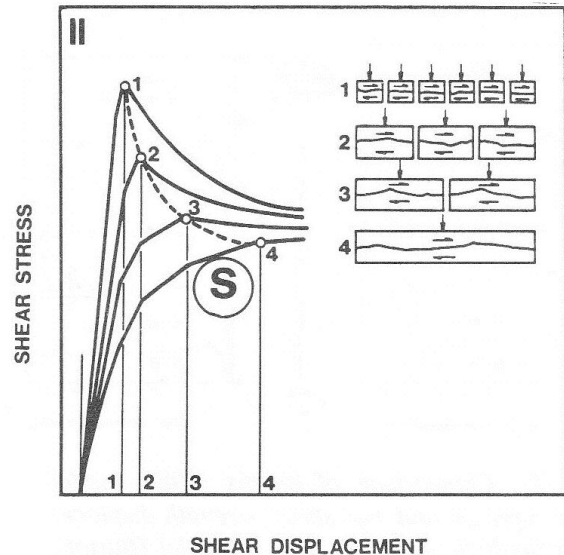


Fig. 11. The shear (*S*) component of rock joint behaviour (Bandis et al., 1981)

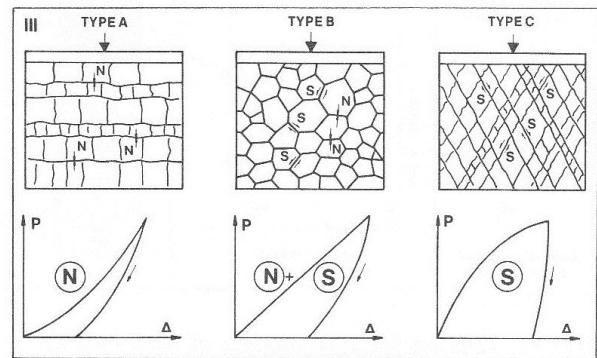


Fig. 12. Predicted load-displacement behaviour of rock masses as a function of the components *N* and *S* (Barton, 1985)

8. PHYSICAL MODELS OF OVERSTRESSED BOREHOLES

The failure of the intact rock surrounding boreholes that are drilled in overstressed rock is complex primarily due to the behaviour of the fractured material resulting from the failure. Maury (1987) has emphasised that the failure of the intact rock may initiate inside the walls of the borehole, due perhaps to stress dependent deformation moduli of the micro-cracked material. Bandis et al. (1987) have shown that peak tangential stresses also occur inside the walls of the borehole. Carefully instrumented blocks of model material were drilled under three-dimensional stress states, and the approximate location of minimum and maximum tangential

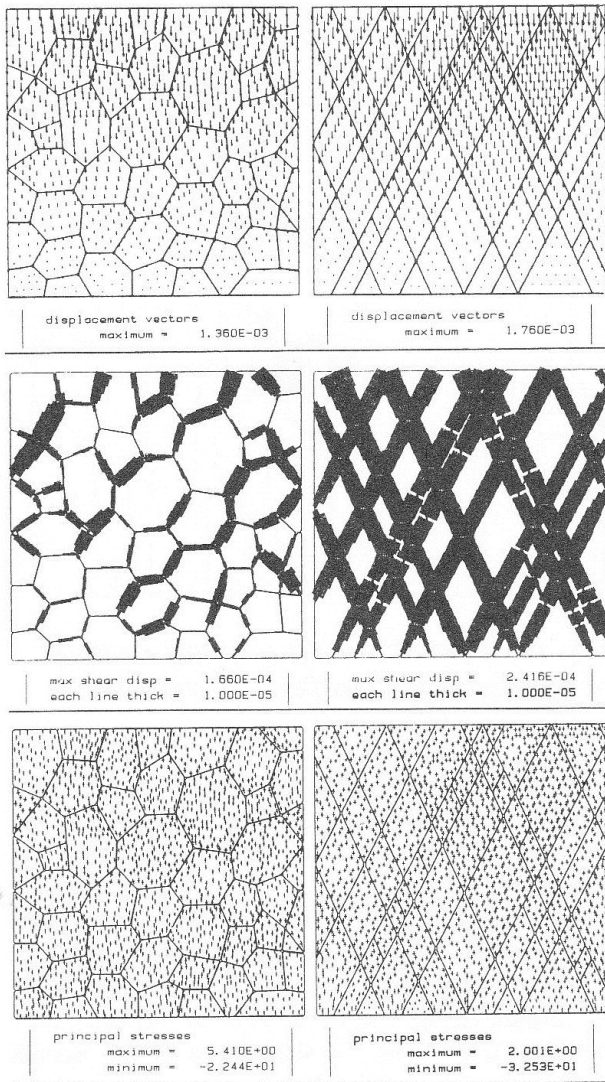


Fig. 13. UDEC-BB model of two-dimensional rock mass response to uniaxial loading (Chryssanthakis et al., 1991)

stresses were recorded during drilling of the hole. The post-failure or rather the "post fracturing" behaviour of the borehole wall material is of greatest interest in the present context, because the failure mode appears to be determined by whether the fractures developed are dilatant or not (Barton, 1987). The two basic failure modes identified by Maury (1987) shown in Fig. 14, are likely to show non-dilatant shearing in the case of the log-spiral shearing, but dilatant extensional behaviour in the case of less plastic and more brittle rock types.

The log-spiral type failure surfaces noted by Bandis et al. (1986) and shown in Fig. 15, may bear little resemblance to the plastic zones predicted by continuum analysis. One of the reasons for this may be due to the fact that the log-spiral

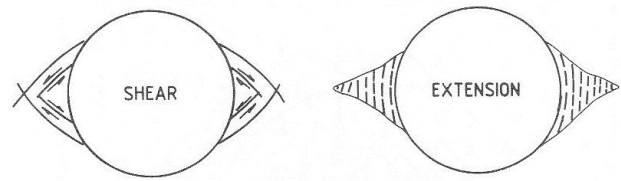


Fig. 14. Two basic failure modes for boreholes in "plastic" and "brittle" rock (after Maury, 1987)

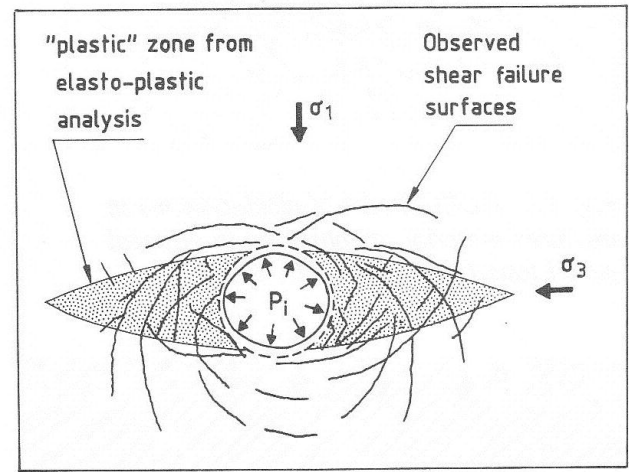


Fig. 15. Comparison of shear failure surfaces observed in a physical model with the plastic zone predicted analytically. (Bandis et al., 1986)



Fig. 16. Model borehole drilled at 45° to σ_1 and σ_3 , but perpendicular to σ_2 . (Addis et al., 1990)

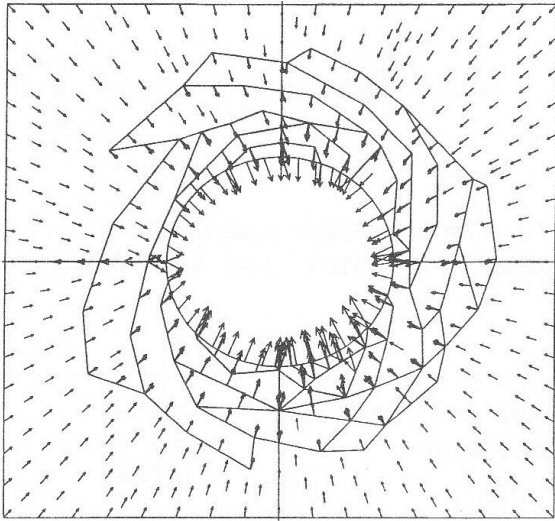


Fig. 17. UDEC model of displacements in fractured material, as observed in physical model tests (Rawlings et al., 1993)

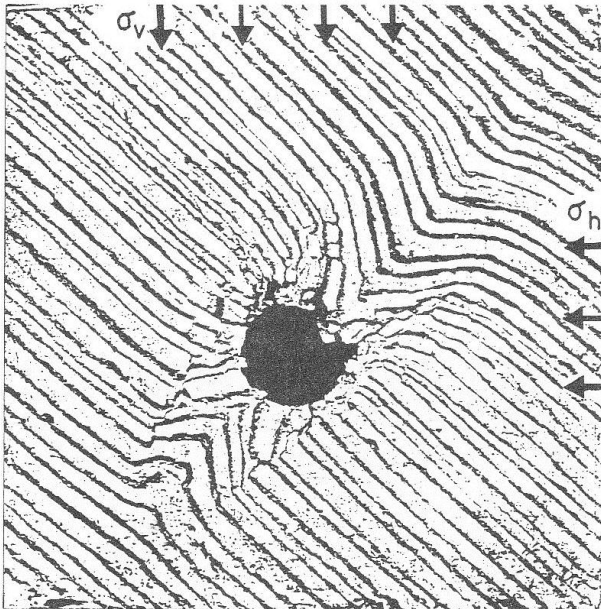


Fig. 18. Deep propagation of displacements in a highly stressed layered medium (Bandis, 1990)

failure surfaces physically shear, thereby "protecting" the intact rock from further distress due to the stress redistribution. An example from NGI's physical model tests of deviated boreholes drilled under stress (Fig. 16) shows clear evidence of offset of a primary family of log-spiral surfaces as a second set develops, due presumably to the stress redistribution caused by yielding on the first set.

Fig. 17 shows recent UDEC modelling of physi-

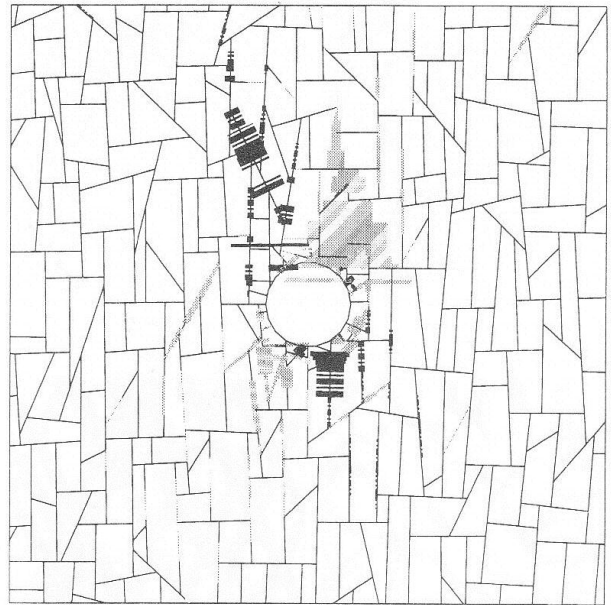


Fig. 19. UDEC-BB model of a shaft excavated in an anisotropic stress field. (Backer, 1993)

cally observed fracturing from NGI's model borehole tests (Rawlings et al., 1993). The mobility of the fractured material (unless retained by mud pressure) is clear.

In many ways the failure of boreholes or tunnels in a medium with pre-existing joints or bedding-induced anisotropy is more straightforward. Nevertheless, the size of the zone of influence may be surprising. Fig. 18 shows one of the Bandis (1990) model excavations in a weak, layered, highly stressed material. There is obvious stress and displacement influence to a depth of some three or four diameters.

When stress anisotropy causes low or negative values of minimum tangential stress, the disturbance in the form of joint aperture changes or joint shearing may be even deeper seated than the above, as shown in one of NGI's UDEC-BB models, Fig. 19 (Backer, 1993).

9. FAILURE MODES IN TUNNELS

The failure modes experienced in tunnels and larger excavations are dependent on the local presence or absence of unfavourably oriented jointing, weak layers, etc. Wagner (1987) gives a useful summary of some of the more common failure modes observed in highly stressed mine openings, as reproduced in Fig. 20. Many of the failures illustrated involved failure of the intact rock in spite of, or sometimes because of, the

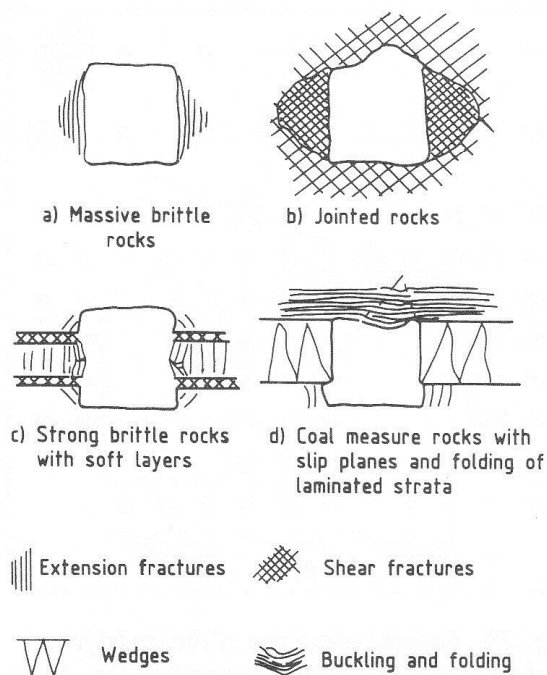


Fig. 20. Typical failures in highly stressed mine openings, after Wagner (1987).

presence of weak layers.

At much shallower depth, the modes of failure of tunnels are dominated by movement along the joint planes. Usually this is stimulated by the presence, within the same opening, of low strength non-dilatant (perhaps contractant) joint or discontinuity infillings. The four cases shown in Fig. 21 from Cecil (1975) demonstrate the likely modes of failure (translational shear or block rotation).

A key feature of model rock mass behaviour noted by Barton and Bandis (1982) is that a threshold block size appears to exist below which block rotation appears to occur in preference to translational shear. The model, idealised rock masses illustrated in Fig. 8 always showed rotational shear when as many as 4,000 blocks were involved, but not when there were 1,000 or less blocks.

10. PHYSICAL MODELS OF LARGE CAVERNS

Physical models simulating rock slope excavation in 40,000 block models and cavern excavation in 20,000 block models have been described by Barton (1971) and Barton and Hansteen (1979). The models were constructed of slabs of tension-fractured, weak, brittle model material using the

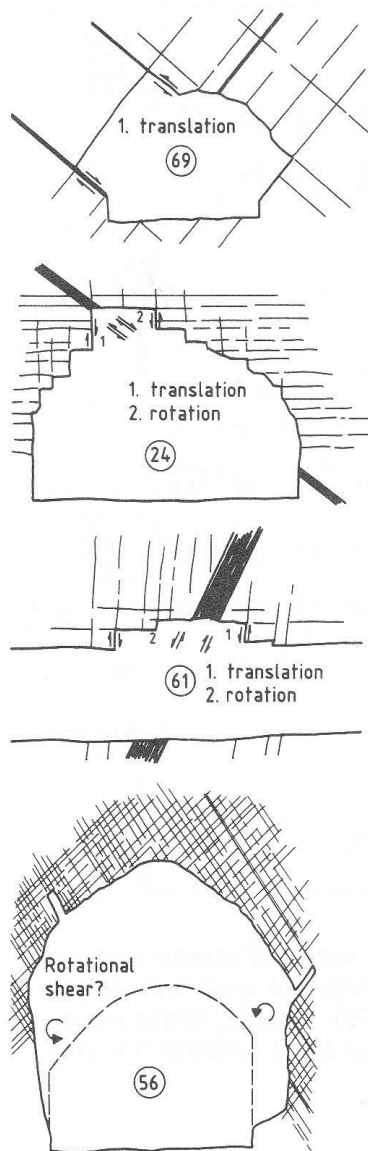


Fig. 21. Four examples of tunnel overbreak or partial failure, caused by translational shear along clay bearing discontinuities or rotational shear in the case of small block sizes. (After Cecil, 1975; Barton, 1987)

same double-bladed guillotine technique used to develop the individual tension fractures and multiple fractured slabs of model material depicted in Figs 1 and 8. The two-dimensional models were loaded by gravity and by either low or relatively high levels of applied horizontal stress.

Fig. 22 shows the displacement vectors recorded for two of the models of large 50m span near-surface caverns. These formed part of a Norwegian study for investigating the feasibility of siting nuclear power plan reactor vessels underground.

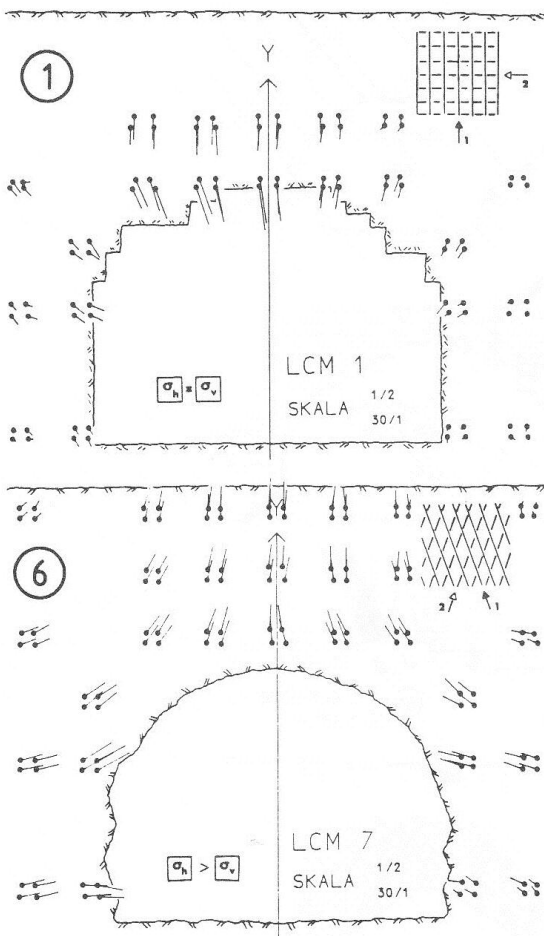


Fig. 22. Physical models of caverns excavated in low and high horizontal stress fields (Barton and Hansteen, 1979). (Model jointing shown to correct scale; set No. 1 guillotine-fractured first.

Strong contrasts in behaviour were caused both by the two different levels of horizontal stress, and by the four different joint patterns investigated under unchanged stress levels.

An example of twin-cavern excavation and an induced faulting event (50mm shearing at full scale) is shown in Fig. 23. Increased shearing and general vertical consolidation of the 20,000 block model was noted following subsequent model earthquake load simulation (Barton and Hansteen, 1979).

11. DISCRETE ELEMENT MODELLING OF LARGE CAVERNS

The physical model studies of large caverns shown in the previous section, and related FEM studies (Barton and Hansteen, 1979) indicated that

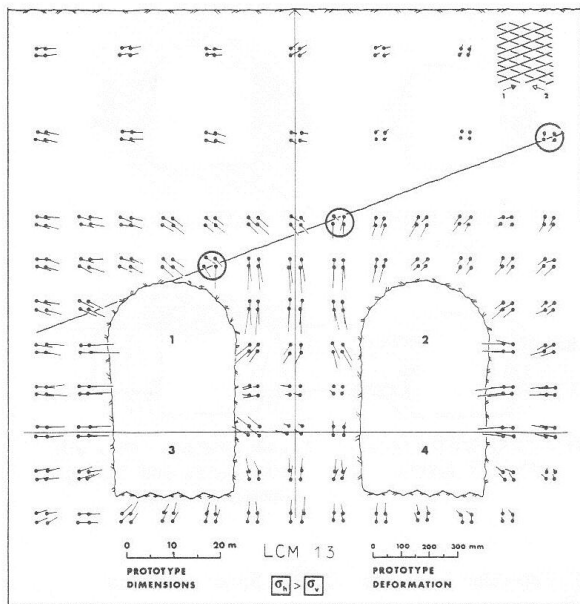


Fig. 23. Faulting along one of the model joint surfaces caused by twin cavern excavation, at stage No. 3. (Barton and Hansteen, 1979)

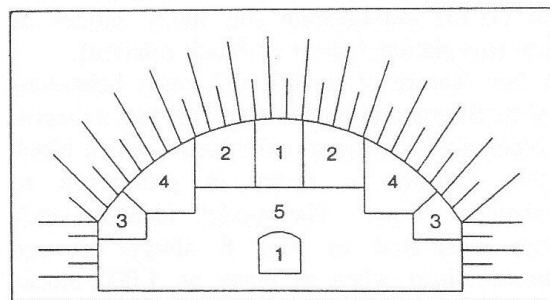
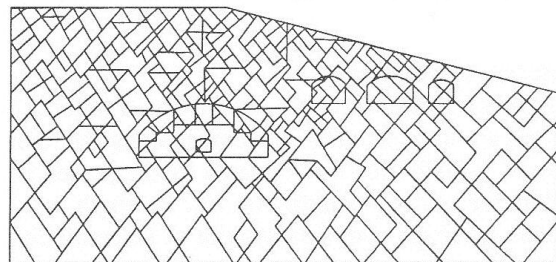


Fig. 24. Assumed joint geometry, bolting pattern and excavation order for modelling the Gjøvik cavern (Chryssanthakis et al., 1992).

large caverns could in certain circumstances demonstrate very small arch deformations. A certain combination of cavern span, depth below surface and horizontal stress level (preferably high) could result almost in balance between downward and upward displacements.

Preliminary discrete element UDEC-BB scoping

studies for the 62m span Olympic Ice Hockey cavern, recently constructed at Gjøvik for the 1994 Winter Olympic Games showed the extreme importance of high horizontal stress levels. Maximum arch displacements (all downwards) were 19.2, 8.4 and 4.0mm with ratios of horizontal stress to vertical stress of 0.5, 1 and 3. (Measured stresses later proved to be nearly $K = 3$.)

Figs 24 and 25 illustrate some of the final stages of modelling with predictions of vertical displacements in the range 5 to 7mm. Total measured displacements were in the range 7 to 8mm, and included the surface subsidence of approximately 3mm (Barton et al., 1992). The prediction and measurements are so close that this case record can almost be considered as a validation of the UDEC-BB code, and its ability to model excavation effects in jointed rock.

REFERENCES

- Addis, M.A., N. Barton, S.C. Bandis and J.P. Henry, 1990, "Laboratory studies on the stability of vertical and deviated boreholes", 65th Annual Technical Conference and Exhibition of the Society of Petroleum Engineers, New Orleans, September 23-26, 1990.
- Backer, L., 1993. Private communication.
- Bandis, S., 1980, "Experimental studies of scale effects on shear strength, and deformation of rock joints. Ph.D. Thesis, Univ. of Leeds, England, 385 p.
- Bandis, S., A. Lumsden and N. Barton, 1981, "Experimental studies of scale effects on the shear behaviour of rock joints", *Int. J. of Rock Mech. Min. Sci. and Geomech. Abstr.* 18, pp. 1-21.
- Bandis, S., A.C. Lumsden and N. Barton, 1983, "Fundamentals of Rock Joint Deformation", *Int. J. Rock Mech. Min. Sci. and Geomech. Abstr.* Vol 20, No. 6, pp. 249-268.
- Bandis, S.C., F. Nadim, J. Lindman, and N. Barton, 1986, "Stability investigations of modelled rock caverns at great depth". *Proc., International Symposium on Large Rock Caverns, Helsinki, Finland, 25-28 Aug.*
- Bandis, S., J. Lindman and N. Barton, 1987, "Three-dimensional stress state and fracturing around cavities in overstressed weak rock", *Proc. of 6th ISRM Congress, Montreal, Canada. Vol. 2, pp. 769-775.*
- Bandis, S.C., 1990, "Fracture modes around tunnels in weak rocks". *Proc. of Int. Conf. "Le Rocce Tenere", Torino, Italy, Ed. G.*

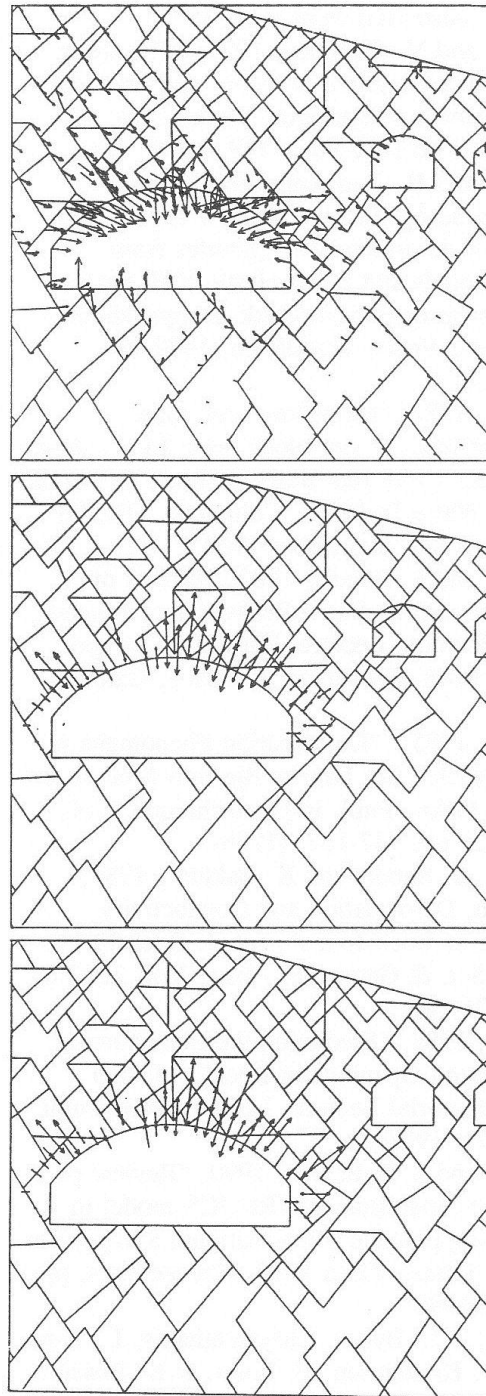


Fig. 25. Displacement vectors (maximum downwards vector = 7.0mm) and bolt forces. (Chryssanthakis et al., 1992)

- Barla, SGE, Padova, pp. 12.1-12.10.
- Barton, N., 1971, "A model study of the behaviour of steep excavated rock slopes", Ph.D. Thesis, Univ. of London.
- Barton, N., 1976, "The shear strength of rock and rock joints", *Int. Jour. Rock Mech. Min. Sci. and Geomech. Abstr.*, Vol. 13, No. 9, pp.

- 255-279. Also NGI-Publ. 119, 1978.
- Barton, N. and V. Choubey, 1977, "The shear strength of rock joints in theory and practice", *Rock Mechanics*, Springer, Vienna, No. 1/2, pp. 1-54. Also NGI-Publ. 119, 1978.
- Barton, N. and H. Hansteen. 1978, "Large underground openings at shallow depth: Comparison of deformation magnitudes from jointed models and linear elastic F.E. analyses", *Fjellsprengningsteknikk, Bergmekanikk*, Oslo, Tapir Press, Trondheim, 1979, pp. 20.1-20.30.
- Barton, N., 1982, "Modelling rock joint behaviour from in situ block tests: Implications for nuclear waste repository design", Office of Nuclear Waste Isolation, Columbus, OH, 96 p., ONWI-308, September 1982.
- Barton, N. and S. Bandis, 1982, "Effects of Block Size on the Shear Behaviour of Jointed Rock", Keynote Lecture, 23rd U.S. Symposium on Rock Mechanics, Berkeley, California.
- Barton, N., 1985, "Deformation Phenomena in Jointed Rock", 8th Laurits Bjerrum Memorial Lecture, Oslo. Publ. in *Geotechnique*, Vol. 36, No. 2, pp. 147-167, (1986).
- Barton, N., S. Bandis and K. Bakhtar, 1985, "Strength, Deformation and Conductivity Coupling of Rock Joints", *Int. J. Rock Mech. & Min. Sci. & Geomech. Abstr.* Vol. 22, No. 3, pp. 121-140.
- Barton, N., 1987, "Predicting the Behaviour of Underground Openings in Rock", Manuel Rocha Memorial Lecture, Lisbon. NGI Publication 172, 1988.
- Barton, N. and S.C. Bandis, 1990, "Review of predictive capabilities of JRC-JCS model in engineering practice", International Symposium on Rock Joints. Loen 1990. Proceedings, pp. 603-610, 1990.
- Barton, N., T.L. By, P. Chryssanthakis, L. Tunbridge, J. Kristiansen, F. Løset, R.K. Bhasin, H. Westerdahl and G. Vik, 1992, "Comparison of prediction and performance for a 62m span sports hall in jointed gneiss". International Conf., Torino, Italy, Ed. G. Barla, pp. 17.1-17.15.
- Cecil, O.S., 1975, "Correlations of rock bolt-shotcrete support and rock quality parameters in Scandinavian tunnels". *Swedish Geotech. Inst. Proc. No. 27*, Stockholm, 275p.
- Chryssanthakis, P., K. Monsen and N. Barton, 1991, "Tunnelling in jointed rock simulated in a computer" (In Norwegian). *Tunneller og Undergrunnsanlegg*, 1989-1991, NTNF, Oslo, pp. 23-28.
- Chryssanthakis, P. and N. Barton, 1992, "Predicting performance of the 62m span ice hockey cavern in Gjøvik, Norway", *Proc. of Int. Con. Fractured and Jointed Rock Masses*, Lake Tahoe, CA, Preprints, LBL, 32379, Vol. 3.
- Cundall, P.A., 1980, "A generalized distinct element program for modelling jointed rock. Report PCAR-1-80. Peter Cundall Associates; Contract DAJA37-79-C-0548, European Research Office, U.S. Army.
- Hardin, E.L., N. Barton, R. Lingle, M.P. Board and M.D. Voegele, 1981, "A heated flatjack test series to measure the thermomechanical and transport properties of in situ rock masses", Office of Nuclear Waste Isolation, Columbus, OH, ONWI-260, 193 p.
- Hart, R.D., Cundall, P.A. and Cramer, M.L., 1985, "Analysis of a loading test on a large basalt block". *Proc. 26th US Symp on Rock Mechanics*, Rapid City SD, 26-28 June 1985, pp. 759-768.
- Hoek, E., 1983, "Strength of jointed rock masses", 23rd Rankine Lecture, *Geotechnique*, Vol. 33, No.3, pp. 187-223.
- Ladanyi, B. and G. Archambault, 1972, "Evaluation de la resistance au cisaillement d'un massif rocheux fragmente". *Proc. 24th Int. Geol. Congr. Montreal. Sec. 130*, pp. 249-260.
- Maury, V., 1987, "Observations, recherches and recent results about failure mechanisms around single galleries". *Proceedings of the 6th ISRM International Congress, Montreal, Canada*, Vol. 2: pp. 1119-1128.
- Rawlings, C.G., N. Barton, S.C. Bandis, M.A. Addis and M. Gutierrez, 1993, "Laboratory Numerical and Discontinuum Modelling of Wellbore Stability During Drilling in Low Permeability Reservoirs". Paper to be presented at the SPE Rocky Mountain Regional/Low Permeability Reservoirs Symposium, Denver, CO, 26-28 April 1993.
- Rocha, M., 1964, "Mechanical Behaviour of Rock Foundations in Concrete Dams", *Intl. Cong. on Large Dams*, 8, Edinburgh, Transactions, Vol. 1, pp. 785-831.
- Wagner, H., 1987, "Design and Support of underground excavations in highly stressed rock". Keynote paper, *Proc. of 6th ISRM Congress, Montreal*.